

Interface-induced magnetism in perovskite quantum wells

Clayton A. Jackson and Susanne Stemmer

Materials Department, University of California, Santa Barbara, California 93106-5050, USA

(Received 9 July 2013; published 19 November 2013)

We investigate the angular dependence of the magnetoresistance of thin (<1 nm), metallic SrTiO₃ quantum wells epitaxially embedded in insulating, ferrimagnetic GdTiO₃ and insulating, antiferromagnetic SmTiO₃, respectively. The SrTiO₃ quantum wells contain a high density of mobile electrons ($\sim 7 \times 10^{14}$ cm⁻²). We show that the longitudinal and transverse magnetoresistance in the structures with GdTiO₃ are consistent with anisotropic magnetoresistance, and thus indicative of induced ferromagnetism in the SrTiO₃, rather than a nonequilibrium proximity effect. Comparison with the structures with antiferromagnetic SmTiO₃ shows that the properties of thin SrTiO₃ quantum wells can be tuned to obtain magnetic states that do not exist in the bulk material.

DOI: [10.1103/PhysRevB.88.180403](https://doi.org/10.1103/PhysRevB.88.180403)

PACS number(s): 75.75.-c, 75.30.Gw, 75.70.-i, 77.84.Bw

Proximity effects at interfaces between ferromagnetic insulators and conductors with strong spin-orbit coupling have attracted attention as components of hybrid structures for spintronics, quantum computing, and as a route to Majorana fermions.¹⁻³ Oxide heterostructures are particularly attractive for inducing phenomena through interfacial proximity, because the relevant phenomena, such as superconductivity, spin-orbit coupling, two-dimensional electron gases, and magnetism can all be found in a single materials class, the perovskites, allowing for high-quality epitaxial structures.

A prototypical perovskite heterostructure is that between the ferrimagnetic Mott insulator GdTiO₃, and the band insulator SrTiO₃. Such interfaces exhibit a high-density, two-dimensional electron gas (2DEG) with $\sim 3 \times 10^{14}$ cm⁻² mobile carriers in the SrTiO₃.⁴ Thin (<2 nm) quantum wells of SrTiO₃ embedded in GdTiO₃ show magnetoresistance hysteresis at low temperatures.⁵ It was suggested that the proximity to the ferrimagnetic GdTiO₃ likely plays a role, but the magnetic state of the SrTiO₃ was not resolved. For example, it is possible that the SrTiO₃ quantum well has become magnetic due to exchange coupling. Theoretical calculations suggest a tendency towards ferromagnetism for thin quantum wells.^{6,7} In this case, the SrTiO₃ quantum well may exhibit magnetotransport properties typical of ferromagnets, such as anisotropic magnetoresistance (AMR). An alternative explanation is that the resistance hysteresis reflects the orientation of the magnetization in the GdTiO₃, without the SrTiO₃ quantum well itself being ferromagnetic. The latter is a nonequilibrium proximity effect that has become known as spin Hall magnetoresistance (SMR), and results from a combination of direct and inverse spin Hall effects.⁸⁻¹⁰ Spin-orbit coupling is at the core of both SMR and AMR. As spin-related effects are important in both bulk SrTiO₃ (Ref. 11) and SrTiO₃ 2DEGs,^{12,13} either AMR (for a ferromagnetic quantum well) or SMR (for a nonmagnetic quantum well) may occur. The two phenomena are distinguishable by the dependence of the magnetoresistance on the orientation of the magnetic field.⁸

To engineer novel states at interfaces between conducting, nonmagnetic perovskites and insulating, magnetic perovskites, it is essential that the magnetic state of these interfaces be understood. In this Rapid Communication, we report angular-

dependent magnetoresistance studies of narrow SrTiO₃ quantum wells, embedded in ferrimagnetic GdTiO₃ and antiferromagnetic SmTiO₃, respectively. The results are consistent with exchange coupling-induced ferromagnetism in the SrTiO₃ in case of interfaces with GdTiO₃ and, more indirectly, with induced antiferromagnetism in the case of SmTiO₃.

GdTiO₃/SrTiO₃/GdTiO₃ quantum well structures were grown by hybrid molecular beam epitaxy on (001) (LaAlO₃)_{0.3}(Sr₂AlTaO₆)_{0.7} (LSAT) crystals. The data reported here are for a sample with 4-nm top and bottom GdTiO₃ layers, and 0.8-nm SrTiO₃ (about three SrO layers¹⁴). Samples of SmTiO₃/SrTiO₃/SmTiO₃ with varying SrTiO₃ thicknesses were also investigated. In both samples, the SrTiO₃ quantum wells are metallic and contain a high, mobile carrier density ($\sim 7 \times 10^{14}$ cm⁻²), due to interface doping from each interface.⁴ In contrast to GdTiO₃, which is ferrimagnetic with a Curie temperature of ~ 30 K in bulk¹⁵ and ~ 20 K in the samples with 4-nm GdTiO₃,⁵ SmTiO₃ is antiferromagnetic with a Néel temperature of ~ 50 K.¹⁶ Electrical and structural characterization, as well as growth details have been described elsewhere.^{5,14,17,18} The carrier mobility was an order of magnitude higher than in conducting, doped GdTiO₃ or SmTiO₃, showing that electrical transport occurs only in the SrTiO₃ quantum well [further evidence comes from magnetotransport; Seebeck measurements, which are SrTiO₃-like;¹⁹ and the band offsets, which favor charge transfer into the SrTiO₃ (Refs. 4 and 20)].

Electrical contacts were deposited by electron beam evaporation in van der Pauw geometry with a shadow mask and consisted of 40-nm Ti/400-nm Au, with the Au contact being the topmost layer. Magnetoresistance and Hall data were collected using a Physical Property Measurement System (Quantum Design PPMS Dynacool). The system's resistivity option was used for Hall and sheet resistance and the electrical transport option for magnetoresistance. The latter utilizes an internal lock-in technique with a frequency of 70.1 Hz and an averaging time of 20 s per measurement. An external junction box allows assigning any function to any contact pad using external cables, and was used to confirm that the same behavior was measured within each possible contact geometry for a specific measurement geometry. The magnetoresistance was measured between ± 1 T, pausing every 0.016 T to

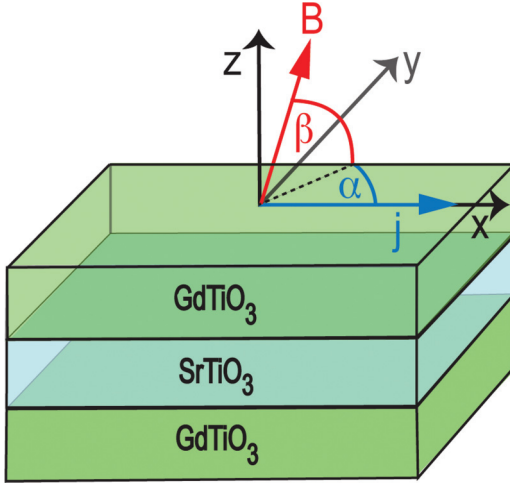


FIG. 1. (Color online) Schematic of the measurement geometry, where \mathbf{j} indicates the current, α is the in-plane angle between \mathbf{B} and \mathbf{j} , and β is the out-of-plane angle. The SrTiO₃ quantum well is sandwiched between two GdTiO₃ layers, epitaxially grown on LSAT.

collect data using the internal lock-in. The sweep rate between data collection points was 0.015 T/s. Multiple sweep rates were checked and no noticeable difference was detected. Longer averaging times showed no appreciable change in the resistance measurement. The angular dependence of the magnetoresistance was characterized by varying the angles α and β between the current, \mathbf{j} , and the magnetic field, \mathbf{B} . As shown in Fig. 1, α lies in the film plane ($\alpha = 0^\circ$ for \mathbf{B} and \mathbf{j} parallel), while β is the angle between the film plane and \mathbf{B} ($\beta = 0^\circ$ if \mathbf{B} lies in the film plane). To vary β , a horizontal rotator was used. The angle α was set to 0° or 90° by rotating the external leads, and to 45° by adjusting the placement of the sample on the mounting puck.

The overall longitudinal magnetoresistance (R_{xx}) of all samples, including SmTiO₃/SrTiO₃/SmTiO₃, was negative at low temperatures, independent of whether the field was in or out of plane. This is contrary to what is expected for weak localization of a two-dimensional system, which is one possible origin of negative magnetoresistance. Negative magnetoresistance can, however, also be due to ferromagnetism or antiferromagnetism of the 2DEG.^{21,22} However, only the GdTiO₃/SrTiO₃/GdTiO₃ samples exhibited magnetoresistance hysteresis, which was superimposed on the slowly varying negative R_{xx} background [see Fig. 2(a)]. The onset temperature for the hysteresis is about 5 K.²³ Thus the presence of the ferrimagnetic GdTiO₃ is a necessary requirement for ferromagnetism in these samples.

Figure 2 shows the relative changes of R_{xx} and transverse magnetoresistance (planar Hall, R_{xy}), respectively, for the GdTiO₃/SrTiO₃/GdTiO₃ quantum well structure for three different values of α , at $\beta = 0^\circ$. Hysteretic behavior is observed for all α , except for $\alpha = 0^\circ$ in the planar Hall geometry. Both the transverse and the longitudinal hysteresis show a crossover from dip to peak behavior with α . The relative changes are larger in R_{xy} , where the peak for $\alpha = 45^\circ$ corresponds to a $\sim 20\%$ change. The absolute resistance changes are, however, comparable.

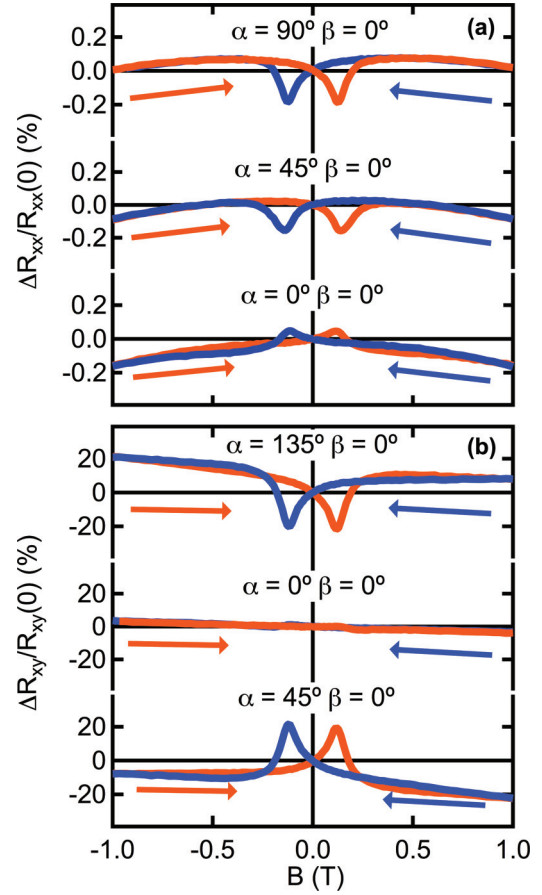


FIG. 2. (Color online) (a) Relative changes in the longitudinal magnetoresistance as a function of in-plane angle α , at $\beta = 0^\circ$. $\Delta R_{xx} = R_{xx}(B) - R_{xx}(0)$, where $R_{xx}(0)$ is the resistance at zero magnetic field. (b) Relative changes in the transverse magnetoresistance as a function of in-plane angle α , at $\beta = 0^\circ$. $\Delta R_{xy} = R_{xy}(B) - R_{xy}(0)$, where $R_{xx}(0)$ is the resistance at zero magnetic field. All measurements are at 2 K.

To distinguish between SMR and AMR, we note that the resistivity changes as a function of magnetization orientation for the two effects are described by^{8,24,25}

$$\text{SMR: } \rho_{xx} = \rho_0 - \Delta\rho_S m_y^2, \quad \rho_{xy} = \Delta\rho_S m_x m_y, \quad (1)$$

$$\text{AMR: } \rho_{xx} = \rho_\perp + \Delta\rho_A m_x^2, \quad \rho_{xy} = \Delta\rho_A m_x m_y. \quad (2)$$

Here, ρ_{xx} and ρ_{xy} are the longitudinal and transverse resistivities, ρ_0 is a constant,²⁴ and $\Delta\rho_S$ and $\Delta\rho_A$ are the resistivity changes for the SMR and AMR, respectively. $\Delta\rho_A = \rho_{\parallel} - \rho_{\perp}$, where ρ_{\parallel} and ρ_{\perp} are the resistivities with the field parallel and perpendicular to the current, respectively. The components of the magnetization along the x and y axes are $m_x = \cos \alpha \cos \beta$ and $m_y = \sin \alpha \cos \beta$. It is clear [Eq. (1)] that R_{xx} for $\beta = 0^\circ$ does not behave according to the SMR effect, because the R_{xx} should be maximized for $\alpha = 0^\circ$ and minimized for $\alpha = 90^\circ$, as $\Delta\rho_S > 0$ always applies.²⁴ The experimental behavior is opposite, namely, at large fields, when the magnetization should be parallel to \mathbf{B} , R_{xx} decreases for $\alpha = 0^\circ$ and increases for $\alpha = 90^\circ$ [Fig. 2(a)]. Instead, R_{xx} at $\beta = 0^\circ$ follows AMR behavior with $\Delta\rho_A < 0$, for which the resistance should be maximized for $\alpha = 90^\circ$ and minimized $\alpha = 0^\circ$ [Eq. (2)], as is

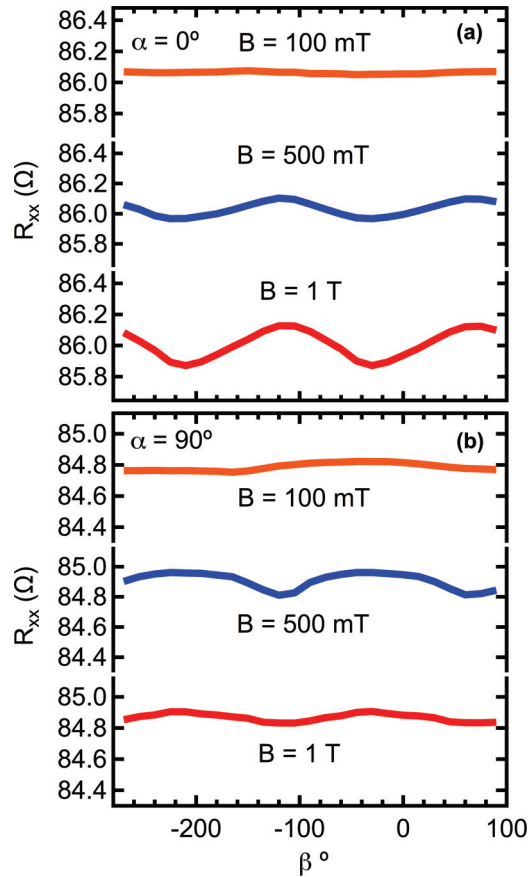


FIG. 3. (Color online) Angular out-of-plane (β) dependence of R_{xx} at three different B fields for (a) $\alpha = 0^\circ$ and (b) $\alpha = 90^\circ$. All measurements are at 2 K.

indeed observed. R_{xy} at $\beta = 0^\circ$ is also consistent with AMR and $\Delta\rho_A < 0$. In this case, R_{xy} should be maximized (positive) for $\alpha = 135^\circ$, minimized (negative) for $\alpha = 45^\circ$, and zero for $\alpha = 0^\circ$, exactly as is observed [see Fig. 2(b)].

The two effects can be further distinguished by measuring the change in resistance as the magnetization is rotated out of plane, at a fixed α . Figure 3 shows the β -angle dependence of R_{xx} for $\alpha = 0^\circ$ and $\alpha = 90^\circ$, respectively, at three different values of B . For AMR, $\Delta\rho_A < 0$, and $\alpha = 0^\circ$ we expect a cosine dependence on β , with R_{xx} increasing, as β is increased, which is observed when B exceeds the demagnetization field [see Fig. 3(a)]. In contrast, for SMR, R_{xx} should be independent of β for $\alpha = 0^\circ$. The behavior at $\alpha = 90^\circ$ is more complicated, because it shows a β -angle dependence [Fig. 3(b)]. For AMR and $\alpha = 90^\circ$, R_{xx} should be independent of β . It is, however, also inconsistent with SMR, for which changing β away from 0° should cause R_{xx} to increase, not decrease, as is observed. The anisotropy in R_{xx} at $\alpha = 90^\circ$ thus has a different origin, and most likely reflects the two-dimensionality of the system, which may also contribute to the offset seen for $\alpha = 0^\circ$ [Fig. 3(a)], i.e., the minimum of R_{xx} is shifted slightly from $\beta = 0^\circ$. The $\text{SmTiO}_3/\text{SrTiO}_3/\text{SmTiO}_3$ quantum well structure also shows a decrease in R_{xx} as β is changed from 0° to 90° for $\alpha = 90^\circ$ (see Fig. 4), confirming that the anisotropy is independent of ferromagnetism.

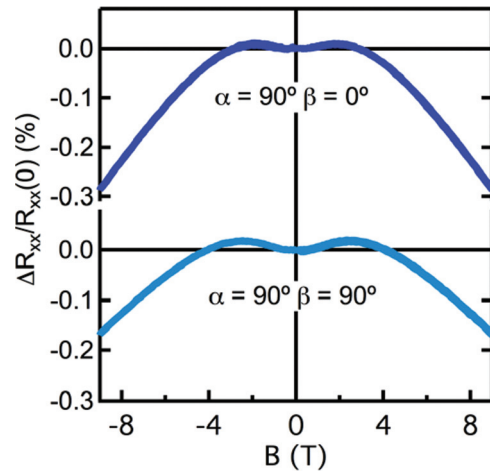


FIG. 4. (Color online) Relative changes in the longitudinal magnetoresistance for a $\text{SmTiO}_3/\text{SrTiO}_3/\text{SmTiO}_3$ sample for $\alpha = 90^\circ$ and $\beta = 90^\circ$ (bottom) and $\beta = 0^\circ$ (top), respectively. The SmTiO_3 layer thicknesses are 10 nm and the SrTiO_3 layer thickness is 0.4 nm. The field was swept from positive B to negative B , and back. No hysteresis is observed.

The occurrence of AMR demonstrates that the SrTiO_3 quantum wells in the $\text{GdTiO}_3/\text{SrTiO}_3/\text{GdTiO}_3$ structures are themselves ferromagnetic. The results also provide evidence for the importance of spin-orbit coupling in these SrTiO_3 quantum wells, which is necessary for AMR. The ferromagnetism is a result of exchange coupling, as it does not appear in quantum wells bound by SmTiO_3 . The origin of the negative AMR ($\Delta\rho_A < 0$) requires further theoretical investigations into the microscopic mechanisms, but there may be similarities to compressively strained, two-dimensional, magnetic III-V semiconductors, which show negative AMR.²⁶ We note that the SrTiO_3 quantum wells are under compressive strain from the LSAT substrate. The fact that the AMR is relatively weak may explain why an anomalous Hall effect could not be detected.²³

The ferromagnetic properties of the quantum well are clearly distinct from those of the GdTiO_3 . For example, at 2 K, the coercive field of the GdTiO_3 in these samples is about 0.02 T,⁵ whereas the dips/peaks in the magnetoresistance of the quantum wells appear at around 0.1 T. The onset of hysteresis in the quantum wells occurs near ~ 5 K, whereas the Curie temperature of the 4-nm GdTiO_3 is ~ 20 K. We also note that ferromagnetism and metallic conduction do not coexist in the rare earth titanates.²⁷ Octahedral distortions, a requirement for ferromagnetism in the *insulating* rare earth titanates,²⁸ do not appear until the quantum wells are thinner than those investigated here, and insulating.¹⁴

We hope that these results provide an incentive for future theoretical studies that examine the relative role of different parameters (exchange, orbital character of the occupied subbands in the SrTiO_3 , and carrier density) in the magnetism, its dependence on the thickness of the quantum well, and its microscopic nature.²⁹ Because the magnetism is induced by a ferromagnetic insulator, which does not interfere with electrical transport, the structures show potential for combining correlated phenomena and engineering novel states of matter. The nearly isotropic negative magnetoresistance

for the quantum wells embedded in SmTiO_3 suggests that proximity effects allow for inducing antiferromagnetism as well.

The authors gratefully acknowledge Gerrit Bauer, Jim Allen, Ezekiel Johnston-Halperin, and Leon Balents for very helpful discussions. The work was supported by a MURI program of the Army Research Office (Grant No. W911-NF-09-1-0398) and DARPA (Grant No. W911NF-12-1-0574). C.A.J.

also received support from the National Science Foundation through a Graduate Research Fellowship. Acquisition of the oxide MBE system used in this study was made possible through an NSF MRI grant (Award No. DMR 1126455). The work made use of central facilities of the UCSB MRL, which is supported by the MRSEC Program of the National Science Foundation under Award No. DMR-1121053. The work also made use of the UCSB Nanofabrication Facility, a part of the NSF-funded NNIN network.

-
- ¹J. D. Sau, R. M. Lutchyn, S. Tewari, and S. Das Sarma, *Phys. Rev. Lett.* **104**, 040502 (2010).
- ²A. Brataas, *Physics* **6**, 56 (2013).
- ³J. Alicea, *Rep. Prog. Phys.* **75**, 076501 (2012).
- ⁴P. Moetakef, T. A. Cain, D. G. Ouellette, J. Y. Zhang, D. O. Klenov, A. Janotti, C. G. Van de Walle, S. Rajan, S. J. Allen, and S. Stemmer, *Appl. Phys. Lett.* **99**, 232116 (2011).
- ⁵P. Moetakef, J. R. Williams, D. G. Ouellette, A. P. Kajdos, D. Goldhaber-Gordon, S. J. Allen, and S. Stemmer, *Phys. Rev. X* **2**, 021014 (2012).
- ⁶R. Chen, S. B. Lee, and L. Balents, *Phys. Rev. B* **87**, 161119(R) (2013).
- ⁷S. Okamoto and A. J. Millis, *Nature* **428**, 630 (2004).
- ⁸H. Nakayama, M. Althammer, Y.-T. Chen, K. Uchida, Y. Kajiwara, D. Kikuchi, T. Ohtani, S. Geprägs, M. Opel, S. Takahashi, R. Gross, G. E. W. Bauer, S. T. B. Goennenwein, and E. Saitoh, *Phys. Rev. Lett.* **110**, 206601 (2013).
- ⁹N. Vlietstra, J. Shan, V. Castel, B. J. van Wees, and J. Ben Youssef, *Phys. Rev. B* **87**, 184421 (2013).
- ¹⁰C. Hahn, G. de Loubens, O. Klein, M. Viret, V. V. Naletov, and J. Ben Youssef, *Phys. Rev. B* **87**, 174417 (2013).
- ¹¹H. Uwe, T. Sakudo, and H. Yamaguchi, *Jpn. J. Appl. Phys.* **24**, 519 (1985).
- ¹²A. D. Caviglia, M. Gabay, S. Gariglio, N. Reyren, C. Cancellieri, and J. M. Triscone, *Phys. Rev. Lett.* **104**, 126803 (2010).
- ¹³G. Khalsa, B. Lee, and A. H. MacDonald, *Phys. Rev. B* **88**, 041302(R) (2013).
- ¹⁴J. Y. Zhang, J. Hwang, S. Raghavan, and S. Stemmer, *Phys. Rev. Lett.* **110**, 256401 (2013).
- ¹⁵H. D. Zhou and J. B. Goodenough, *J. Phys.: Condens. Matter* **17**, 7395 (2005).
- ¹⁶A. C. Komarek, H. Roth, M. Cwik, W. D. Stein, J. Baier, M. Kriener, F. Bouree, T. Lorenz, and M. Braden, *Phys. Rev. B* **75**, 224402 (2007).
- ¹⁷P. Moetakef, C. A. Jackson, J. Hwang, L. Balents, S. J. Allen, and S. Stemmer, *Phys. Rev. B* **86**, 201102(R) (2012).
- ¹⁸P. Moetakef, J. Y. Zhang, S. Raghavan, A. P. Kajdos, and S. Stemmer, *J. Vac. Sci. Technol. A* **31**, 041503 (2013).
- ¹⁹T. A. Cain, S. Lee, P. Moetakef, L. Balents, S. Stemmer, and S. J. Allen, *Appl. Phys. Lett.* **100**, 161601 (2012).
- ²⁰G. Conti *et al.*, *J. Appl. Phys.* **113**, 143704 (2013).
- ²¹I. Garate, J. Sinova, T. Jungwirth, and A. H. MacDonald, *Phys. Rev. B* **79**, 155207 (2009).
- ²²V. K. Dugaev, P. Bruno, and J. Barnas, *Phys. Rev. B* **64**, 144423 (2001).
- ²³See Supplemental Material at <http://link.aps.org/supplemental/10.1103/PhysRevB.88.180403> for Hall effect measurements and for temperature-dependent magnetoresistance data.
- ²⁴Y. T. Chen, S. Takahashi, H. Nakayama, M. Althammer, S. T. B. Goennenwein, E. Saitoh, and G. E. W. Bauer, *Phys. Rev. B* **87**, 144411 (2013).
- ²⁵T. R. McGuire and R. I. Potter, *IEEE Trans. Magn.* **11**, 1018 (1975).
- ²⁶T. Jungwirth, M. Abolfath, J. Sinova, J. Kučera, and A. H. MacDonald, *Appl. Phys. Lett.* **81**, 4029 (2002).
- ²⁷F. Iga, T. Naka, T. Matsumoto, N. Shirakawa, K. Murata, and Y. Nishihara, *Physica B* **223-224**, 526 (1996).
- ²⁸M. Mochizuki and M. Imada, *Phys. Rev. Lett.* **91**, 167203 (2003).
- ²⁹X. Li, W. V. Liu, and L. Balents, arXiv:1308.4179 [cond-mat.str-el] (2013).